Journal of Sound and Vibration 325 (2009) 769–780

Contents lists available at ScienceDirect

Journal of Sound and Vibration

journal homepage: www.elsevier.com/locate/jsvi

The whistling potentiality of an orifice in a confined flow using an energetic criterion

P. Testud [a,1], Y. Aurégan [b], P. Moussou [a,*], A. Hirschberg [c]

[a] Laboratoire de Mécanique des Structures Industrielles Durables, UMR CNRS-EDF 2832, 1 Avenue du Général De Gaulle, F-92141 Clamart, France
[b] Laboratoire d'Acoustique de l'Université du Maine, UMR CNRS 6613, Avenue Olivier Messiaen, F-72085 Le Mans Cedex 9, France
[c] Fluid Dynamics Laboratory, Department of Applied Physics, Technische Universiteit Eindhoven, P.O. Box 513, 5600 MB Eindhoven, The Netherlands

ARTICLE INFO

Article history:
Received 17 July 2007
Received in revised form
27 March 2009
Accepted 30 March 2009
Handling Editor: C.L. Morfey
Available online 21 May 2009

ABSTRACT

Using a two-source method, the scattering matrices of 10 sharp-edged thin orifices are measured under different subsonic flow conditions. The data are analysed in terms of net acoustical energy balance: the potential whistling frequency range is defined as the one associated with acoustical energy production.

A Strouhal number describing the maximum whistling potentiality is found to be equal to 0.2–0.35, based on the orifice thickness and the orifice jet velocity. It appears to depend on the Reynolds number and on the ratio of orifice to pipe diameters.

Tests are performed to compare theoretically and experimentally the potential whistling frequency to the actual whistling frequency. They are found to coincide within the measurement uncertainty.

1. Introduction

Flow singularities such as valves, taps and orifices are present in large number in industrial pipe systems. In certain conditions of flow regimes, singularities like single-hole orifices are known to sometimes whistle. This phenomenon is not taken into account at the design stage, because its occurrence is quite occasional. When it occurs, a high level of vibration can be generated with a risk of fatigue failure, or a high level of noise can be generated outside the pipe, causing acoustic nuisance to workers in the installations and to people in the vicinity.

A detailed description of self-sustained oscillations can be found in the literature [1–4]: the whistling phenomenon is known to be related to the instability of the shear flow, associated with an hydrodynamic feedback or with an acoustic feedback. Hydrodynamic feedback occurs when the vortices generated along the shear layer reach an area where the steady velocity exhibits a gradient, as for instance if an abrupt expansion is present downstream the shear layer. Feedback can happen as well in reverberating acoustic conditions. In both cases, the feedback velocity fluctuation modulates the vorticity in the shear layers, and energy is transferred from the main flow to self-sustained oscillations. The whistling dominated by hydrodynamic direct feedback, such as the edge-tone, is most extensively discussed by Refs. [5–9]. Acoustically driven oscillation in cavities have been extensively studied by, among others, Refs. [1,10–14]. The whistling of an orifice in a confined flow with acoustical reflecting conditions has been investigated by Rockwell [6] and Anderson [15–21]. Vortex shedding in a very thick orifice is described in Ref. [22]. A whistling orifice in an industrial configuration is reported in Ref. [23].

* Corresponding author. Tel.: +33 1 47 65 44 43; fax: +33 1 47 65 36 92.
E-mail address: pierre.moussou@edf.fr (P. Moussou).
[1] Currently with ASTRIUM, France.

0022-460X/$ - see front matter © 2009 Elsevier Ltd. All rights reserved.
doi:10.1016/j.jsv.2009.03.046

In the first part, the linear response of a non-whistling orifice determined by means of a two-source method is investigated, in a manner similar to recent experiments [24]. The whistling potentiality of an orifice is experimentally determined from its scattering matrix, rewritten in terms of net production of acoustical energy. A Strouhal frequency associated with the maximum of whistling potentiality is obtained from measurements on 10 sharp-edge orifices with different pipe flows.

In the second part, the actual whistling of an orifice is investigated by arranging it inside a pipe terminated by acoustical reflectors, forming an acoustical resonator. The whistling frequencies are compared to the potential whistling frequencies. The neutral stability of the system is studied by using a linear model incorporating the measured scattering matrix for the orifice.

2. Theoretical criterion for the whistling ability of an orifice

A theoretical criterion for the whistling ability of a flow singularity has been proposed in Ref. [25], based on the acoustic energy balance of the incipient and of the scattered acoustic waves measured in non-whistling conditions. The definition of acoustic energy in steady flows has been given by Morfey [26], and it can be shown that the energy balance expression requires the use of the so-called exergy waves [27], defined by

$$\Pi^{\pm} = (1 \pm M_0)p^{\pm}, \tag{1}$$

where M_0 is the Mach number of the steady flow in the pipe, $p^{\pm}$ is the propagating pressure, the $+$ sign stands for propagation in the flow direction and the $-$ sign stands for propagation in the reverse direction.

Considering incipient and scattered pressure waves in the harmonic regime, one defines the exergy scattering matrix of an orifice as a 2×2 complex matrix:

$$\begin{pmatrix} \Pi_2^+ \\ \Pi_1^- \end{pmatrix} = \mathbf{S_e} \begin{pmatrix} \Pi_1^+ \\ \Pi_2^- \end{pmatrix}. \tag{2}$$

Let the acoustic energy production of the orifice be characterized by a dimensionless number, equal to the difference of the incipient and of the scattered acoustic power, divided by the incipient power. Due to energy properties, this ratio is a real number, and it can be shown [25] that its higher and lower possible values are the eigenvalues of the matrix $\mathbf{I} - \mathbf{S_e^* S_e}$, where the star stands for the complex conjugate. The criterion can be expressed the following way: an orifice is prone to whistling in adequate acoustic conditions if one of the eigenvalues is negative, because the orifice can amplify acoustic waves. The other way around, if both eigenvalues are positive, the orifice never whistles.

It is worth mentioning the fact that such a linear criterion provides only instability frequencies, and not the actual whistling frequencies. In self-sustained oscillation regime, nonlinear effects occur which stabilize the amplitude of the pressure oscillations, and there is no theoretical reason why the whistling frequency should match the instability frequency. From an experimental point of view, the literature reports that the whistling frequency is often close to the linear instability frequency, but does not coincide [28,29]. As will be seen, this is the case in the present study.

3. Experimental procedure

In order to experimentally determine the coefficients of the exergy scattering matrix of the previous section, the forward and backward pressure propagating waves need be measured using the two-microphone method. The test section consists of a straight pipe with an inner diameter D equal to 30 mm and a total length of 6 m (see Fig. 1), with quasi-anechoic terminations arranged upstream and downstream of the measurement area. Acoustic pressures are measured upstream and downstream of the orifice by two series of four microphones B&K 4938 with Nexus 2690 amplifiers; the distances between successive sensors are, respectively, 63.5, 211.5 and 700 mm in order to optimize the identification of propagating pressure waves. A fully automated system determines the incipient and scattered propagating pressure waves using a two-source method [30,31]: the loudspeaker frequency ranges from 400 to 5000 Hz with steps of 10 Hz, at each change of frequency, a settling time of 1000 cycles is used to establish the response, and the measurement is made over a period of 1000 cycles. More details about the rig and the measurement procedure can be found in Refs. [32,30,33]. The duct

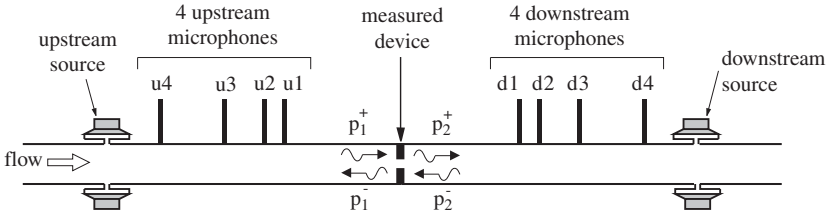

Fig. 1. The measurement zone: from both sides of the orifice, four fluctuating pressure transducers and an excitation source are used.

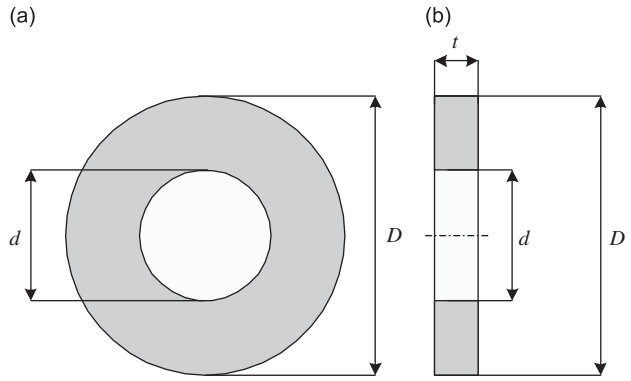

Fig. 2. Scheme of the sharp angle orifices: circular-centred, single-holed, without bevel: (a) front view and (b) side view.

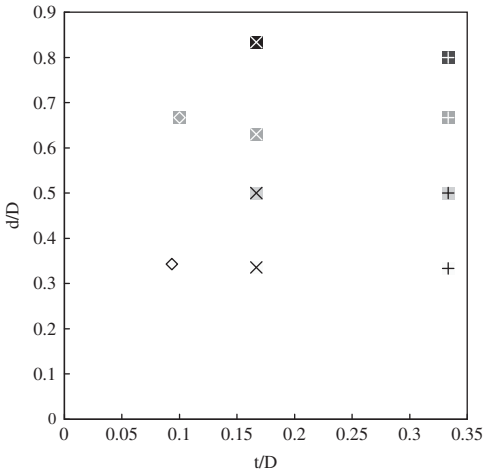

Fig. 3. Geometrical dimensions of the tested orifices.

upstream of the first series of microphones is 2 m long, so that the flow is fully developed. The Reynolds number in the pipe $Re = U_0 D/\nu$ varies from 2×10^3 to 8×10^4, and the pipe Mach number varies from 2.6×10^{-3} to 1.1×10^{-1}.

All tested orifices exhibit a circular centred single hole. Ten orifices have been studied, with sharp angle edges on both sides: an overview of their geometry features is illustrated in Figs. 2 and 3, where the reduced thickness t/D and the reduced inner diameter d/D are plotted. As the thickness-to-inner diameter ratio t/d varies from 0.15 to 1.5, these orifices are thick in the sense of Ref. [34]. Furthermore, one orifice with a bevel on one side was tested.

To ensure the adequacy of the experimental procedure, an evaluation of the influence of the loudspeaker sound level was performed. Nonlinear effects were found to occur when the root mean square of the acoustic velocity exceeded 10% of the steady flow velocity, so that the level of the loudspeaker pressure was set at approximately 130 dB SPL inside the pipe. Moreover, the downstream quasi-anechoic termination was once replaced by an open pipe termination, and the scattering matrix coefficients differed by about $\approx 1\%$, that is, within the experimental margin of error.

4. Instability frequencies of orifices

4.1. Case of a sharp-edge orifice

In this section, results obtained with a sharp-edge orifice with $t/D = 0.17$, $d/D = 0.63$ (▣) and a Mach number equal to 4.2×10^{-2} are discussed. Similar results were obtained with other orifices but for some differences that are discussed in the next section.

The first step consists in determining the ratio of incipient and transmitted propagating pressure waves, as illustrated in Fig. 4. It can already be noted that in the frequency range of 1400–2100 Hz, the scattered pressure waves exhibit a higher value than the incipient ones, so that the orifice behaves as an acoustic amplifier, which is the basis of the instability mechanism. Such an effect is not mentioned in the recent works of Abom et al. [24], because the instability frequency range of the orifice they studied was probably far beyond the loudspeaker frequency range.

As regards the low frequency values of the transmission coefficients, they are consistent with a quasi-stationary model [32,35] using a vena contracta coefficient equal to about 0.7 (see Ref. [36] for more details).

The next step consists in evaluating the eigenvalues and the eigenvectors of $\mathbf{I}-\mathbf{S}_\mathbf{e}^*\mathbf{S}_\mathbf{e}$ as prescribed in Section 2. As can be seen in Fig. 5, one of the eigenvalues is close to zero and the eigenvector associated with the vanishing eigenvalue is such that $\Pi_1^+=\Pi_2^-$ (see Fig. 6); this can be easily explained, because, as long as local compressibility is not at stake, an equal increase of the pressure on both sides of the orifice has no effect on the acoustic velocity. Hence, assuming the pressure to be close to the exergy for low Mach numbers, and the acoustic velocity variation being equal to zero on each side of the orifice, the upstream and downstream pressures are equal. If the incipient exergy waves are such that $\Pi_1^+=\Pi_2^-$, one is thus led to the conclusion that $\Pi_1^+=\Pi_2^+$ and $\Pi_1^-=\Pi_2^-$, and the eigenvalue of $\mathbf{I}-\mathbf{S}_\mathbf{e}^*\mathbf{S}_\mathbf{e}$ is zero.

The other way around, the other eigenvalue becomes negative in the frequency range of 1400–2100 Hz, highlighting the whistling ability of this orifice. The eigenvector associated with the non-vanishing eigenvalue is such that $\Pi_1^+=-\Pi_2^-$ (see Fig. 7). This corresponds to an excitation of the orifice by a velocity fluctuation, which is classically known to best enhance vortex shedding (see for instance Ref. [37]). It is hence possible to evaluate the whistling ability of an orifice by experimentally determining its scattering matrix.

The influence of the flow regime can be investigated with the help of scaling laws for the frequency and for the amplitude of the eigenvalues. The frequency is made dimensionless, introducing a Strouhal number based on the orifice thickness t and the orifice velocity $U_d=U_0\,(D/d)^2$:

$$St=\frac{ft}{U_d}. \tag{3}$$

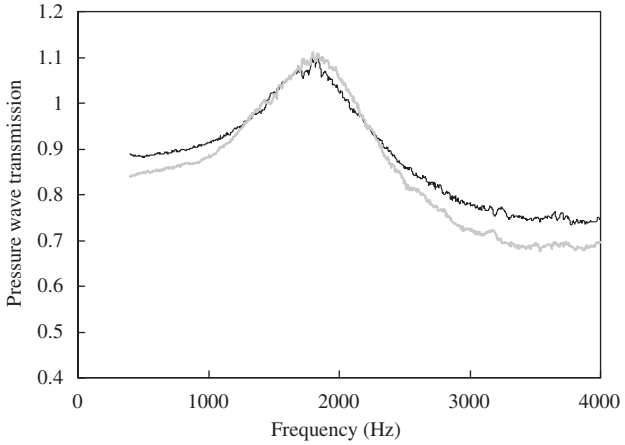

Fig. 4. Absolute value of the ratio of the transmitted and of the incipient propagating pressure waves in the forward (in black) and backward direction (in grey), for a circular centred single-hole orifice (orifice ⊠: $t/D=0.17$, $d/D=0.63$, under $M_0=4.2\times10^{-2}$).

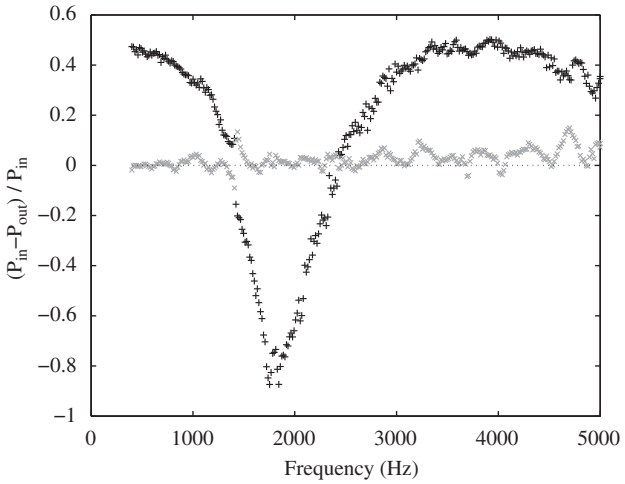

Fig. 5. Eigenvalues representing the ratio of dissipated acoustic power (orifice ⊠: $t/D=0.17$, $d/D=0.63$, under $M_0=4.2\times10^{-2}$). The non-vanishing eigenvalue (black '+') is associated to an excitation in acoustic velocity, whereas the vanishing one (grey '×') is associated to an excitation in acoustic pressure.

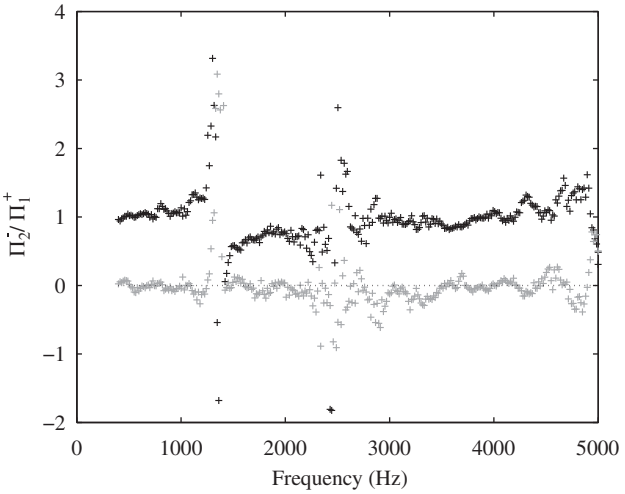

Fig. 6. Amplitude ratio of the eigenvector associated to the vanishing eigenvalue (orifice ▩: $t/D = 0.17$, $d/D = 0.63$, under $M_0 = 4.2 \times 10^{-2}$). Black '+': real part, grey '+': imaginary part.

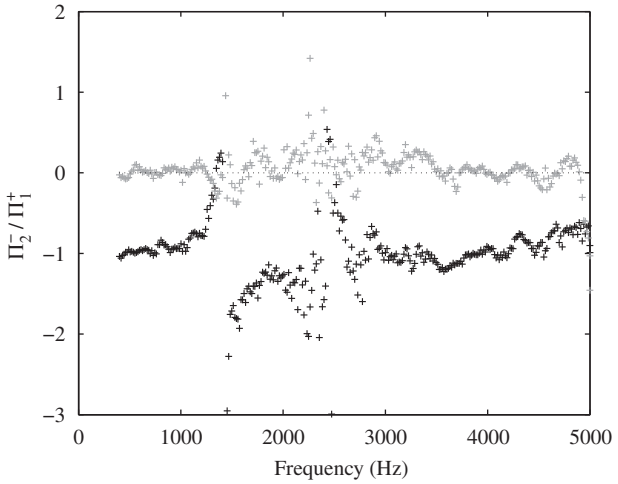

Fig. 7. Amplitude ratio of the eigenvector associated to the non-vanishing eigenvalue (▩, under $M_0 = 4.2 \times 10^{-2}$). Black '+': real part, grey '+': imaginary part.

Other length scalings have been tested and led to a less satisfactory collapse. As regards the eigenvalue amplitude, the best compromise consists in dividing it by the Mach number, yet this empiric scaling would require further work to be fully assessed. As can be seen in Fig. 8, the data collapse reasonably well for the orifice previously studied.

4.2. Behaviour of the other sharp-edge orifices

The other sharp-edge orifices exhibit a behaviour similar to the one of the previous section, but for a few differences. First, it appears that some orifices with a larger thickness exhibit two ranges of frequencies associated with a negative eigenvalue, as shown in Fig. 9. One needs then to take into account the possible existence of higher orders of potential whistling frequencies.

A peak Strouhal number St_p is now defined as being associated with the minimum eigenvalue, related to the first or to the second order of potential whistling frequencies. This Strouhal number is plotted against the pipe Reynolds number $Re = U_0 D/\nu$ in Fig. 10 for all sharp-edge orifices in different flow regimes. For fully turbulent pipe flow ($< Re \gtrsim 5 \times 10^3$), the critical Strouhal numbers obtained for the first mode are in the range 0.2–0.3, in agreement with literature; Ref. [17] indicates a value around 0.26–0.29 for orifices with $0.1 \leqslant t/d \leqslant 0.5$, in a configuration of a free jet (orifice placed at the pipe termination). Furthermore, there seems to exist an effect of the laminar–turbulent transition upon the Strouhal number,

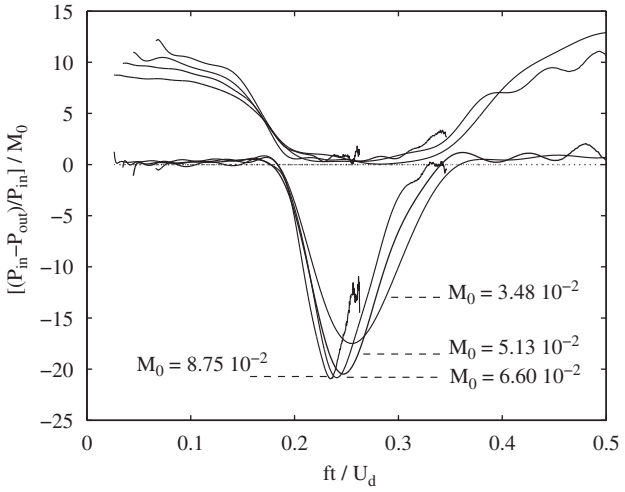

Fig. 8. Eigenvalues scaled with the Mach number in the pipe (orifice ▩: $t/D = 0.17$, $d/D = 0.63$, at different Mach numbers).

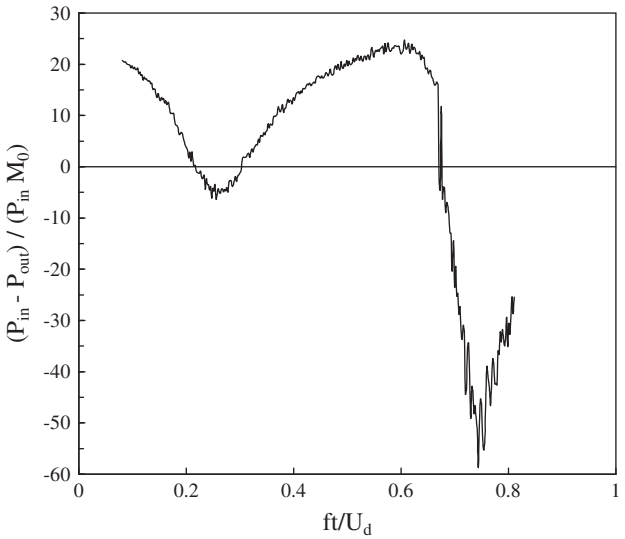

Fig. 9. Non-vanishing eigenvalue of the matrix $\mathbf{I} - \mathbf{S}_e^* \mathbf{S}_e$: two ranges of potentially whistling frequencies are found (orifice ⊞: $t/D = 0.33$, $d/D = 0.5$, under $M_0 = 3.59 \times 10^{-2}$.

which may be related to the variations of the vena contracta section. Blevins [36] indicates that the vena contracta ratio decreases for $d/D = 0.3$ from $\alpha_v = 0.70$ to 0.60 as Re increases from 10^3 to 10^4; for $d/D = 0.7$, the vena contracta ratio decreases from $\alpha_v = 0.81$ to 0.65 as Re increases from 10^3 to 10^4.

Various linear fits on data with multiple parameters have been tested to estimate the dependence of St_p on different parameters: $1/Re^{\beta}$, $\ln(Re)$, $(d/D)^{\beta}$, $(t/d)^{\beta}$, $[D/(D-d)]^{\beta}$, with $\beta > 0$. As a result, it is found that the critical Strouhal number is mainly a function of the Reynolds number Re and the geometrical parameter $D/(D-d)$. For the first hydrodynamic mode, the best linear regression giving the least standard deviation (57% of relative error on 60 data points) is

$$St_p = 0.2420\left(1 + \frac{31.69}{\sqrt{Re}} - 0.0657\frac{D}{D-d}\right), \quad Re \geqslant 5 \times 10^3. \tag{4}$$

4.3. Case of an orifice with a bevel on one side

Literature [4,38] indicates that the presence of a bevel on the upstream side of an orifice enhances its whistling ability whereas a bevel on the downstream side hampers it. In order to test the consistency of the instability criterion, an orifice

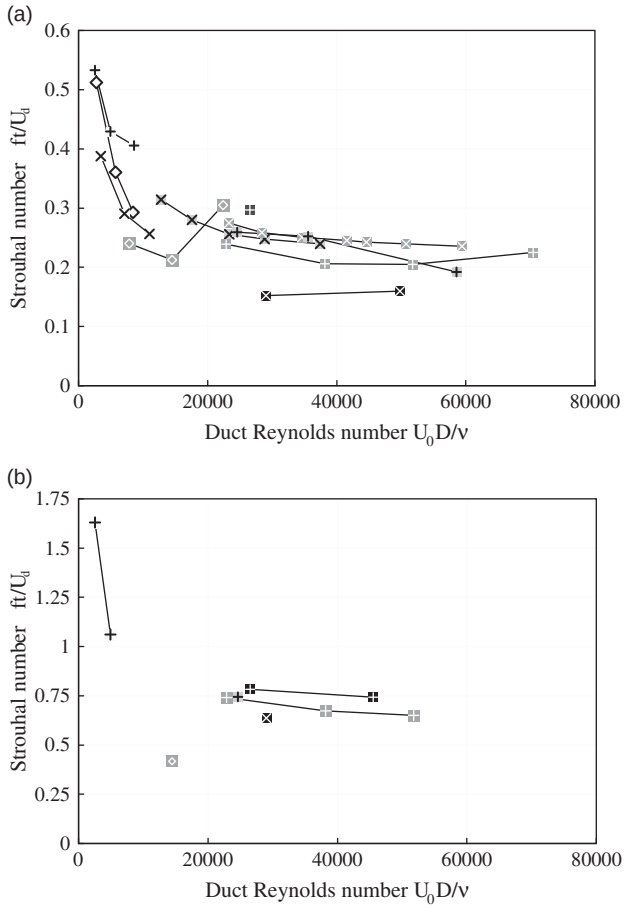

Fig. 10. Strouhal numbers of the first (a) and second (b) peak potentially whistling frequency for different orifices. The series with $t/D = 0.1$ is plotted with diamond markers: $\diamond$ $d/D = 0.34$; $\diamond$ $d/D = 0.66$. The series with $t/D = 0.17$ is plotted with cross markers: $\times$ $d/D = 0.33$; $\times$ $d/D = 0.5$; $\times$ $d/D = 0.63$; $\times$ $d/D = 0.8$. The series with $t/D = 0.33$ is plotted with plus markers: $+$ $d/D = 0.33$; $+$ $d/D = 0.5$; $+$ $d/D = 0.67$; $+$ $d/D = 0.8$.

with a thickness equal to 5 mm, a hole diameter equal to 10 mm and a bevel with a radius equal to 1 mm on one side was made.

The non-vanishing eigenvalues associated with this orifice are plotted in Fig. 11 for a pipe Mach number equal to 7.6×10^{-3}; a potentially whistling frequency range is found when the orifice is arranged bevel upstream, whereas no whistling frequency range is found when the orifice is arranged bevel downstream. Hence, the whistling criterion agrees with classical results.

5. Whistling frequencies of an orifice in a resonant pipe

5.1. Experimental results

In order to validate the criterion, one orifice with a large negative eigenvalue was arranged in a pipe with acoustic reverberating conditions (see Fig. 12). The tested orifice exhibits the following features: $t/D = 0.16$ and $d/D = 0.33$ ($\times$). Acoustic reflecting conditions are arranged from both sides of it, in order to provide the acoustic feedback necessary for whistling. At 0.137 m upstream, an expansion chamber imposes a high reflection coefficient: $|R_u| \approx 0.8$ in the frequency range of 400–2500 Hz, weakly dependent on the flow velocity (see Fig. 13). An absorbing foam is placed inside the expansion chamber to prevent any resonance inside the chamber. At 0.270 m downstream, an unflanged open pipe termination imposes a high reflection coefficient: $|R| > 0.4$ in the frequency range of 400–2500 Hz (see Fig. 14).

One spectrum obtained when whistling occurs is shown in Fig. 15. A sharp peak appears at the whistling frequency, typical of self-sustained oscillations. When increasing the steady flow velocity, the whistling frequency jumps from one acoustic mode to the next one (see Fig. 16), as is classically the case in vortex shedding with lock-in issues. As shown in Fig. 17, whistling frequencies correspond to Strouhal numbers ft/U_d varying from 0.2 to 0.35, i.e., in the range of potential whistling Strouhal numbers described in the former section. No significant difference between the potential and the actual

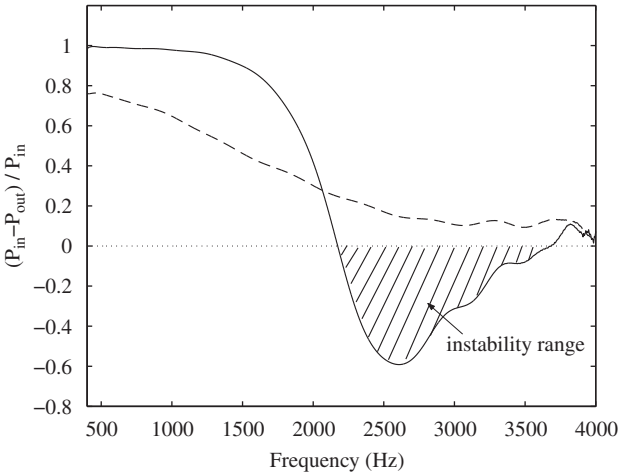

Fig. 11. Influence of the bevel on the evolving eigenvalue: when the bevel is placed at the upstream edge of the orifice, no whistling potentiality is found; when the bevel is placed at the downstream edge of the orifice, a range of potentially whistling frequencies is found (orifice features: $t = 5$ mm, $d = 10$ mm, with a bevel of radius $r_{\text{bevel}} = 1$ mm, under $M_0 = 7.6 \times 10^{-3}$, inside a pipe of inner radius equal to 30 mm). Straight line: bevel downstream, dashed line: bevel upstream.

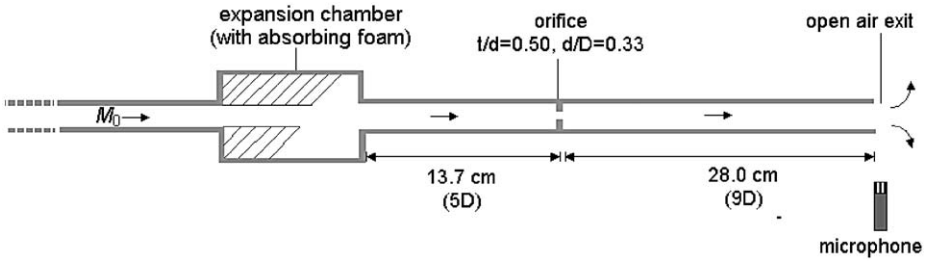

Fig. 12. The studied whistling configuration, constituted by an orifice under steady flow, an expansion chamber upstream and an open pipe termination downstream imposing reflecting conditions. The resulting noise (possibly whistling) is measured by means of a microphone placed outside of the pipe, at the level of the pipe termination, at a distance of 20 cm from the pipe axis.

whistling frequency was observed during the tests, and further work would be needed to determine if this should always be the case.

It is worth mentioning here the fact that the range of Strouhal number observed during the tests is consistent with whistling frequencies observed by Ref. [39] in water in an industrial loop in the presence of cavitation phenomena. This observation suggests that the Strouhal number is neither sensitive to the compressibility of the fluid nor to the presence of cavitation when in water, and that it does not vary significantly when the Reynolds number becomes sufficiently large.

5.2. An attempt to predict the actual whistling frequency

An approximate value of the whistling frequency of an orifice under the effect of a given set of acoustic boundaries can be determined by describing the orifice by its scattering matrix $\mathbf{S_e}$, by describing the boundary conditions by upstream and downstream acoustic reflections coefficients (R_u and R_d, respectively) and by identifying the exergy propagating waves $\Pi^{\pm}$ to the pressure propagating waves $p^{\pm}$. With the notations of Fig. 18, the harmonic regime equations are

$$\begin{pmatrix} 1 & -R_u & 0 & 0 \\ 0 & 0 & -R_d & 1 \\ R_e^+ & -1 & 0 & T_e^- \\ T_e^+ & 0 & -1 & R_e^- \end{pmatrix} \begin{pmatrix} P_1^+ \\ P_1^- \\ P_2^+ \\ P_2^- \end{pmatrix} = \begin{pmatrix} 0 \\ 0 \\ 0 \\ 0 \end{pmatrix}. \tag{5}$$

The whistling frequency is such that non-trivial solutions of Eq. (5) exist. Although frequencies in the complex space should theoretically be looked for, it is assumed here that the whistling frequency is such that the determinant of Eq. (5) comes close to zero for real frequencies. Simplified expressions of the acoustic reflection coefficients are used, namely, upstream (see Fig. 13):

$$R_u = -0.8\, \mathrm{e}^{2\mathrm{j}k(L_u+\delta_u)}, \tag{6}$$

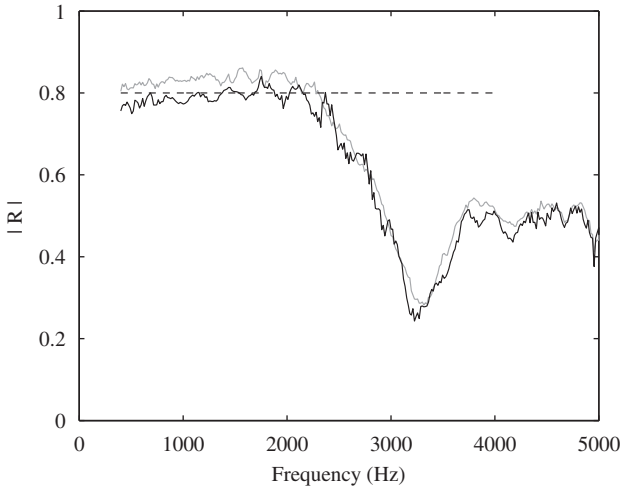

Fig. 13. The upstream reflection coefficient imposed by the expansion chamber, and seen from the orifice. Straight grey line: $M_0 = 5.15 \times 10^{-2}$, straight black line: $M_0 = 7.37 \times 10^{-2}$, dashed black line: value used for the magnitude of R_u.

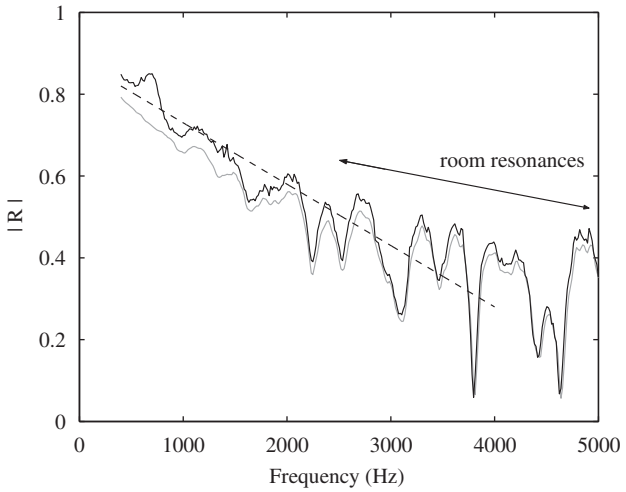

Fig. 14. The downstream reflection coefficient imposed by the expansion chamber, and seen from the orifice. Straight grey line: $M_0 = 0$, straight black line: $M_0 = 4.97 \times 10^{-2}$, dashed black line: value used for the magnitude of R_d for the analytical prediction of the whistling frequency.

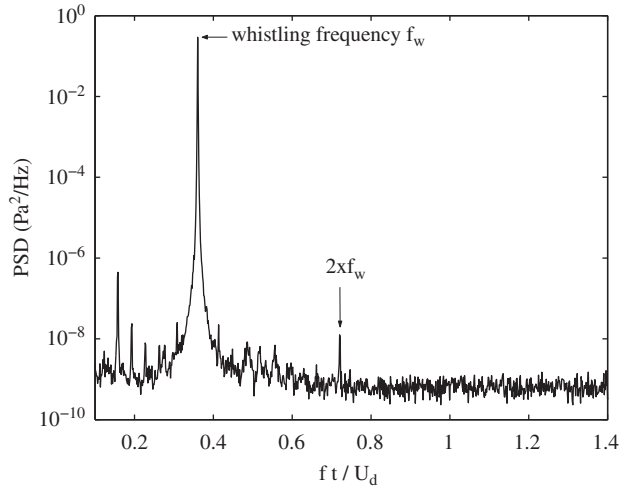

Fig. 15. In the whistling configuration, example of typical pressure power spectrum density obtained far downstream of the orifice (×) ($t/D = 0.16$ and $d/D = 0.33$), exhibiting whistling frequency and harmonics ($M_0 = 4.62 \times 10^{-3}$).

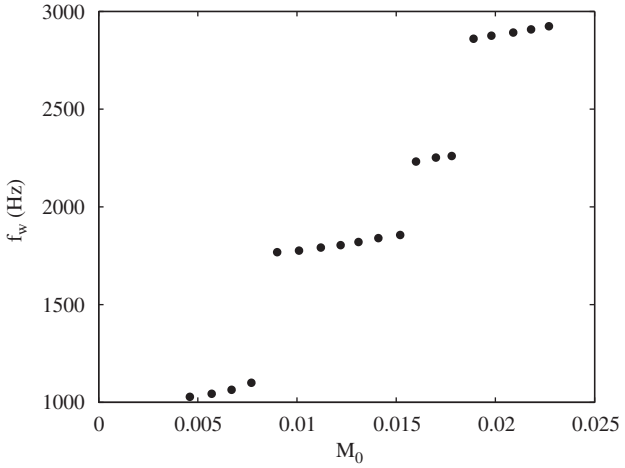

Fig. 16. Whistling frequency as a function of the pipe Mach number, for the orifice (×) ($t/D = 0.16$ and $d/D = 0.33$).

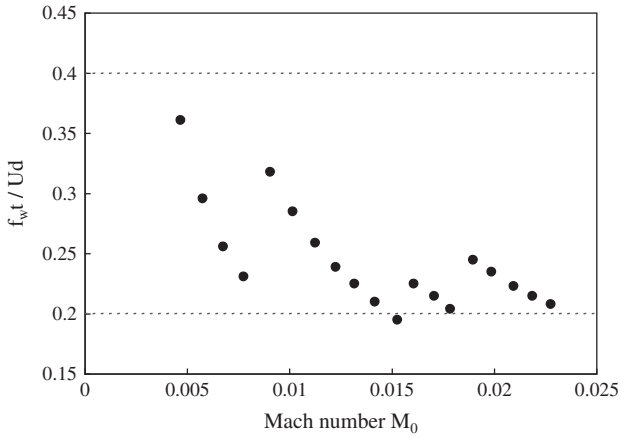

Fig. 17. Whistling Strouhal number as a function of the pipe Mach number, for the orifice (×) ($t/D = 0.16$ and $d/D = 0.33$).

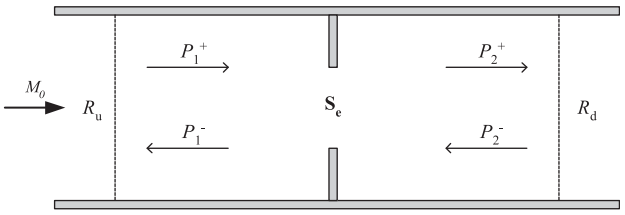

Fig. 18. Scheme of the model to predict the whistling frequency, in the plane wave approximation, using the scattering matrix of the singularity S_e and the acoustic reflection coefficients R_u and R_d, respectively, upstream and downstream of the singularity.

where the plane wavenumber k is associated with the speed of sound c and with the current frequency by $k = 2\pi f/c$, where L_u is the distance between the expansion chamber and the orifice and where $\delta_u = 0.82D/2$ is the end correction of a flanged opening (exit of a duct with infinite baffle, [40]). The downstream acoustic reflection coefficient is (see Fig. 14):

$$R_d = -[0.73 - a(f - f_{\text{ref}})]\, \mathrm{e}^{-2\mathrm{j}k(L_d+\delta_d)}, \tag{7}$$

where L_d is the distance between the orifice and the open end, $a = 1.5 \times 10^{-4}\,\mathrm{Hz}^{-1}$, $f_{\text{ref}} = 1000\,\mathrm{Hz}$ and $\delta_d = 0.61D/2$ corresponds to the end correction of an unflanged opening (exit of a duct with thin walls) at low frequency [41]. The inverse of the determinant obtained using the approximated reflection coefficients and the measured scattering matrix coefficients is plotted in Fig. 19.

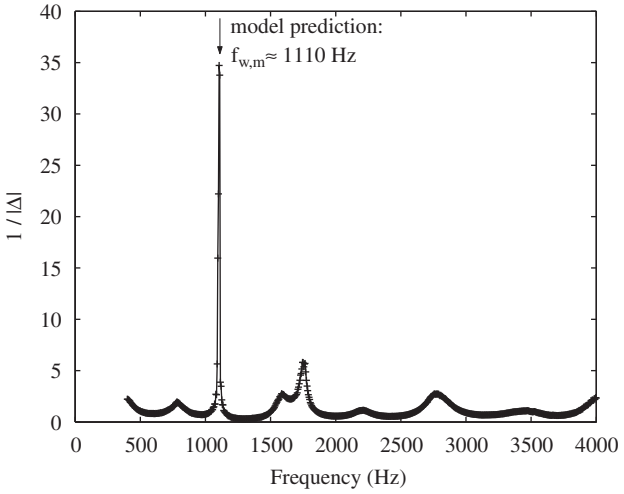

Fig. 19. Study of the vanishing of the magnitude of the determinant of the system to predict the whistling frequencies ($M_0 = 5.2 \times 10^{-3}$).

Despite the approximations, the model gives satisfactory results: the whistling frequency is predicted here within a relative uncertainty of 5%. Furthermore, it can be checked that below a certain amplitude of the reflection coefficients, the model predicts no whistling. Both reflections, upstream and downstream, are necessary to obtain whistling.

6. Conclusion

A two-source method was used to measure the acoustical linear response of orifices under subsonic flow conditions. For given main flow conditions, the net acoustical power generated by the orifices is positive within a certain frequency range. At a given frequency, the highest flow-acoustics interaction occurs when the incipient pressures have opposite phases, as classically observed in the literature.

For sharp-edge orifices, the maximum power generated by the flow passing through the orifice corresponds to a Strouhal number equal to 0.2–0.35, based on the orifice thickness and the orifice flow velocity. This Strouhal number appears to slightly depend on the Reynolds number and on the ratio of orifice to pipe diameters. Potential whistling Strouhal numbers obtained are close to those obtained by Ref. [20] in air (measurements corresponding to low Reynolds numbers), and in water (water flow in weak cavitating condition and high Reynolds number from Ref. [39]).

Tests are performed to compare theoretically and experimentally the potential whistling frequency to the actual whistling frequency. They are found to coincide within the measurement uncertainty.

The theoretical criterion proposed by Auregan and Starobinski is experimentally validated. It can be used to predict the whistling ability of a pressure drop device under the effect of propagating plane pressure waves.

References

[1] D. Rockwell, E. Naudascher, Self-sustained oscillations of impinging free shear layers, *Annual Review of Fluid Mechanics* 11 (1979) 67–94.
[2] W.K. Blake, *Mechanics of Flow-Induced Sound and Vibration*, Academic Press, New York, 1986.
[3] M.S. Howe, *Hydrodynamics and Sound*, Cambridge University Press, Cambridge, 1998.
[4] A. Hirschberg, C. Schram, *A Primitive Approach to Aeroacoustics, Lecture Notes in Physics*, Vol. 586, Springer, Berlin, 2002.
[5] W.K. Blake, A. Powell, *The Development of Contemporary Views of Flow-tone Generation*, Vol. 1, Academic Press, Orlando, 1986.
[6] D. Rockwell, Oscillations of impinging shear layers, *AIAA Journal* 21 (1983) 645–664.
[7] D.G. Crighton, The jet edge-tone feedback cycle—linear theory for the operating stages, *Journal of Fluid Mechanics* 234 (1992) 361–391.
[8] C.M. Ho, N.S. Nossier, Dynamics of an impinging jet, part 1: the feedback phenomenon, *Journal of Fluid Mechanics* 105 (1981) 443–473.
[9] D.S. Weaver, S. Ziada, M.K. Au-Yang, S.S. Chen, M.P. Païdoussis, M.J. Petitgrew, Flow-induced vibration of power and process plant components: progress and prospects, *Journal of Pressure Vessel Technology—Transactions of the ASME* 122 (2000) 339–348.
[10] J.C. Bruggeman, A. Hirschberg, M.E.H. Van Dongen, A.P.J. Wijnands, J. Gorter, Self-sustained aero-acoustic pulsations in gas transport systems: experimental study of the influence of closed side branches, *Journal of Sound and Vibration* 150 (1991) 371–391.
[11] S. Ziada, E.T. Buhlmann, Self-excited resonances of two side-branches in close proximity, *Journal of Fluids and Structures* 6 (1992) 583–601.
[12] S. Dequand, X. Luo, J. Willems, A. Hirschberg, Helmholtz-like resonator self-sustained oscillations, part 1, *AIAA Journal* 41 (3) (2003) 408–415.
[13] A. Billon, étude expérimentale de sons auto-entretenus produits par un jet d'un conduit et heurtant une plaque fendue, Ph.D. Thesis, Université de La Rochelle, 2003.
[14] P. Lafon, S. Caillaud, J.P. Devos, C. Lambert, Aeroacoustical coupling in a ducted shallow cavity and fluid/structure effects on a steam line, *Journal of Fluids and Structures* 18 (6) (2003) 695–713.
[15] A.B.C. Anderson, Dependence of pfeifenton (pipe tone) frequency on pipe length, orifice diameter, and gas discharge pressure, *Journal of the Acoustical Society of America* 24 (1952) 675–681.
[16] A.B.C. Anderson, Dependence of pfeifenton (pipe tone) frequency on pipe-orifice geometry, *Journal of the Acoustical Society of America* 25 (1953) 541–545.

[17] A.B.C. Anderson, A circular-orifice number describing dependency of primary pfeifenton frequency on differential pressure, gas density and orifice geometry, *Journal of the Acoustical Society of America* 4 (1953) 626–631.
[18] A.B.C. Anderson, A jet-tone orifice number for orifices of small thickness-diameter ratio, *Journal of the Acoustical Society of America* 26 (1) (1954) 21–25.
[19] A.B.C. Anderson, Metastable jet-tone states of jets from sharp-edged, circular, pipe-like orifices, *Journal of the Acoustical Society of America* 27 (1) (1955) 13–21.
[20] A.B.C. Anderson, Structure and velocity of the periodic vortex-ring flow pattern of a primary pfeifenton (pipe tone) jet, *Journal of the Acoustical Society of America* 27 (1955) 1048–1053.
[21] A.B.C. Anderson, Vortex ring structure-transition in a jet emitting discrete acoustic frequencies, *Journal of the Acoustical Society of America* 28 (1956) 914–921.
[22] K. Sato, Y. Saito, Unstable cavitation behavior in a circular–cylindrical orifice flow, in *CAV2001, Fourth International Symposium on Cavitation*, California Institute of Technology, Pasadena, USA, 2001 ⟨http://cav2001.library.caltech.edu/318⟩.
[23] P. Moussou, S. Caillaud, V. Villouvier, A. Archer, A. Boyer, B. Rechu, S. Benazet, Vortex-shedding of a multi-hole orifice synchronized to an acoustic cavity in a PWR piping system, in A. Press (Ed.), *ASME PVP Conference*, *No. PVP2003-2086 in PVP-Vol. 465*, *Flow-Induced Vibration*, 2003, pp. 161–168.
[24] M. Abom, S. Allam, S. Boij, Aero-acoustics of flow duct singularities at low mach numbers, in A.I. of Aeronautics, Astronautics (Eds.), *12th AIAA/CEAS Aeroacoustics Conference*, *No. 2687 in AIAA 2006*, 2006, pp. 1–10.
[25] Y. Aurégan, R. Starobinsky, Determination of acoustic energy dissipation/production potentiality from the acoustic transfer functions of a multiport, *Acustica* 85 (1999) 788–792.
[26] C.L. Morfey, Acoustic energy in non-uniform flows, *Journal of Sound and Vibration* 14 (2) (1971) 159–170.
[27] R. Starobinsky, Y. Aurégan, Fluctuations of vorticity and entropy as sources of acoustical exergy, *Journal of Sound and Vibration* 216 (3) (1998) 521–527.
[28] D.H. Fletcher, Air-flow and sound generation in musical and wind instruments, *Annual Review of Fluid Mechanics* 11 (1979) 123–146.
[29] T. Sarpkaya, A critical review of the intrinsic nature of vortex-induced vibrations, *Journal of Fluids and Structures* 19 (2004) 389–447.
[30] Y. Aurégan, M. Leroux, Failures in the discrete models for flow duct with perforations: an experimental investigation, *Journal of Sound and Vibration* 265 (1) (2003) 109–121.
[31] M. Abom, Measurement of the scattering-matrix of acoustical two-port, *Mechanical System and Signal Processing* 5 (1991) 89–104.
[32] G. Ajello, Mesures acoustiques dans les guides d'ondes en présence d'écoulement—mise au point d'un banc de mesure—application à des discontinuités, Ph.D. Thesis, Laboratoire d'Acoustique de l'Université du Maine, Académie de Nantes, 1997.
[33] P. Testud, Aeroacoustics of orifices in confined flow: whistling and cavitation, Ph.D. Thesis, Université du Maine, Académie de Nantes, France, 2006.
[34] I.E. Idelcik, Memento des pertes de charge, Eyrolles, Paris, 1969 (in French).
[35] G. Hofmans, R. Boot, P. Durrieu, Y. Aurégan, A. Hirschberg, Aeroacoustic response of a slit-shaped diaphragm in a pipe at low Helmholtz number, 1: quasi-steady results, *Journal of the Acoustical Society of America* 110 (4) (2000) 1859–1872.
[36] R.D. Blevins, *Applied Fluid Dynamics Handbook*, Krieger, New York, 1984.
[37] M.C. Welsh, G.D.C., Interaction of induced sound with flow past a square leading edged plate in a duct, *Journal of Sound and Vibration* 67 (4) (1979) 501–511.
[38] T.A. Wilson, G.S. Beavers, M.A. De Coster, D.K. Holger, D. Regenfuss, Experiments on the fluid mechanics of whistling, *Journal of the Acoustical Society of America* 50 (1971) 366–372.
[39] P. Testud, P. Moussou, A. Hirschberg, Y. Aurégan, Noise generated by cavitating single-hole and multi-hole orifices in a water pipe, *Journal of Fluids and Structures* 23 (2) (2007) 163–189.
[40] J.W.S. Rayleigh, *The Theory of Sound*, second ed., Vol. 2, Macmillan, New York, 1986.
[41] H. Levine, J. Schwinger, On the radiation of sound from an unflanged circular pipe, *Physical Review* (1948) 383–406.